ATMOSPHERIC SCIENCE LETTERS
Atmos. Sci. Let. **16**: 155–161 (2015)
Published online 21 October 2014 in Wiley Online Library
(wileyonlinelibrary.com) **DOI:** 10.1002/asl2.541

RMetS
Royal Meteorological Society

Influence of the boreal spring Southern Annular Mode on summer surface air temperature over northeast China

Fei Zheng,[1] Jianping Li,[2,3]* Robin T. Clark,[4] Ruiqing Ding,[1] Fei Li[5] and Lei Wang[6,7]

[1]*State Key Laboratory of Numerical Modeling for Atmospheric Sciences and Geophysical Fluid Dynamics, Institute of Atmospheric Physics, Chinese Academy of Sciences, Beijing, China*
[2]*College of Global Change and Earth System Science, Beijing Normal University, China*
[3]*Joint Center for Global Change Studies, Beijing, China*
[4]*Hadley Centre, Met Office, Exeter, UK*
[5]*State Key Laboratory of Atmospheric Boundary Layer Physics and Atmospheric Chemistry, Institute of Atmospheric Physics, Chinese Academy of Sciences, Beijing, China*
[6]*School of Physics, Peking University, Beijing 100871, China*
[7]*Key Laboratory of Research on Marine Hazards Forecasting, National Marine Environmental Forecasting Center, Beijing 100081, China*

**Correspondence to:*
J. Li, College of Global Change and Earth System Science, Beijing Normal University, Beijing 100875, China.
E-mail: ljp@bnu.edu.cn

Received: 15 May 2014
Revised: 18 September 2014
Accepted: 23 September 2014

Abstract

Previous evidence has showed that the boreal spring Southern Annular Mode (SAM) regulates summer monsoon precipitation in East Asian subtropics through the Northern Indian Ocean sea surface temperature (NIO SST). This paper further demonstrates how a positive (negative) boreal spring SAM is usually followed by a warmer (cooler) summer over northeast China (NEC), suggesting impacts of the SAM even extend to the northern mid-latitudes. A positive spring SAM usually leads to anomalous anticyclonic sinking motion over NEC during summer through the NIO SST, which results in cloud reduction and changes in radiation, and thus surface warming.

Keywords: **Southern Annular Mode (SAM); summer surface air temperature; cloudiness; radiation budget**

1. Introduction

The variability of large-scale atmospheric circulation in the Southern Hemisphere (SH) extratropics is dominated by the Southern Annular Mode (SAM), also known as the Antarctic Oscillation (AAO) (Gong and Wang, 1999; Thompson and Wallace, 2000; Li and Wang, 2003). Impact of the SAM however, is not only confined to the SH (Marshall *et al.*, 2004; Ciasto and Thompson, 2008; Yuan and Yonekura, 2011; Simpkins *et al.*, 2012), but also extends to the Northern Hemisphere (NH). For example, a high index value of the boreal spring SAM is commonly followed by a weaker East Asian summer monsoon (EASM) and a wetter summer in the middle and lower reaches of the Yangtze River (Nan and Li, 2003; Nan *et al.*, 2009); a positive phase of the preceding boreal winter SAM usually causes a decrease in spring rainfall over south China (Zheng and Li, 2012). In addition, the SAM also modulates the frequency of boreal summer typhoons over the western North Pacific and West Africa monsoon, and so affects summer precipitation in these regions (Ho *et al.*, 2005; Sun *et al.*, 2010; Choi *et al.*, 2012).

Although the relationship between NH regional precipitation and the SAM has been documented in these earlier studies, little research has been devoted to exploring possible influences of the SAM on NH regional surface air temperature (SAT). Some clues for this kind of influence can be found in the study by Wu *et al.* (2009), which illustrated that the East Asia winter monsoon and boreal winter temperature in China show a robust response to the boreal autumn SAM. However, possible linkages between the SAM and the NH SAT in other seasons are not well understood. As the boreal spring SAM influences the EASM (Nan and Li, 2003; Nan *et al.*, 2009), it seems reasonable to expect a possible connection between the spring SAM and East Asian summer SAT, but this relationship has not been explored in the literature.

This study aims to detect possible influences of the boreal spring SAM on East Asian summer SAT. The specific focus is on the northeast China (NEC), which is at the northern end of the EASM region, as this variability is much stronger than is observed in most other adjacent regions. On the one hand, a cutoff low with a cold center, referred to as the Northeast cold vortex (He *et al.*, 2007), frequently occurs in summer over NEC. On the other hand, summer heat waves are common in NEC (Wu *et al.*, 2012). Therefore, there is increasing concern regarding NEC summer SAT variability, which has been shown to be modulated by many factors including the El Niño–Southern Oscillation (ENSO) (Wu *et al.*, 2010) and North Atlantic sea surface temperatures (SSTs) (Wu *et al.*, 2011). To develop a comprehensive understanding of NEC, summer SAT variability will require investigation of various influencing factors. In view of the little attention that has been paid to identify these influencing factors in the SH, we aim to explore possible influence of the boreal spring SAM on NEC summer SAT.

Besides, as Nan *et al.* (2009) suggested, one underlying factor for the physical process that connects the spring SAM to the East Asian summer circulation is the Indian Ocean SST acting as an oceanic bridge. According to their results, the Indian Ocean SST responds to the spring SAM sequentially from the south to the north, until the SST anomalies finally reach the Northern Indian Ocean (NIO) and influence the EASM. However, they did not provide enough evidence regarding the impacts of the summer NIO SST on the summer East Asian circulation. In view of the importance of the NIO SST for the linkage between the spring SAM and summer East Asian circulation, we also provide new evidence for the role of NIO SST in modulating East Asian circulation.

The remainder of this paper is organized as follows: in Section 2, the data and methodology are briefly described; in Section 3, the linkage between the spring SAM and NEC summer SAT is illustrated, and the corresponding mechanism is given in Section 4. Finally, discussion and conclusions are presented in Section 5.

2. Data and methodology

This study is based on meteorological observations made on a daily basis between 1979 and 2011 at 846 weather stations across China, and includes daily mean, minimum, and maximum SAT; daily mean and minimum relative humidity; precipitation; and sunshine duration (unit: 0.1 h), which is the length of time per day in which the direct solar radiation is greater or equal to 120 W m^{-2}. The monthly atmospheric reanalysis data used were the National Centers for Environmental Prediction (NCEP)/National Center for Atmospheric Research (NCAR) Reanalysis I, which covers the period between 1948 and the present day, and the main variables used include total cloud cover (TCDC), surface net shortwave radiation flux (NSWRF), and surface net longwave radiation flux (NLWRF). Note that the positive sign used in the surface radiation flux data indicates that the direction is upwards; consequently, the NSWRF values are always negative. To display the magnitude of NSWRF most clearly, the sign of NSWRF was reversed. The monthly SST reanalysis data were obtained from the NOAA ERSST V3b. This study focuses on the boreal spring (MAM) and summer (JJA). Prior to analysis, all meteorological elements were converted to seasonal means. The data used here were mainly from the period 1979 to 2011, but went back to 1948 when possible.

The definition of the SAM index (SAMI) developed by Nan and Li (2003) is used here, and is the difference in normalized monthly zonal averaged sea level pressure between 40 and 70°S. The raw monthly SAMI is used to obtain spring seasonal averaged SAMI, and then normalized before analysis. Similarly, the NH Annular Mode (NAM) index (NAMI) is defined as the difference in normalized monthly zonal averaged sea level pressure between 35 and 65°N (Li and Wang, 2003). In addition, the Niño 3.4 index was used to reflect ENSO variability. Singular value decomposition (SVD), correlation, and composite analyses are employed to quantify our results.

3. Linkages between the boreal spring SAM and NEC summer SAT

Correlations between the spring SAM and summer meteorological elements over Northern China are shown in Figure 1. A significant positive correlation between the spring SAM and summer SAT exists in NEC (Figure 1(a); 115–135°E, 40–50°N), indicating that when the spring SAM is in a positive phase, NEC tends to experience a warmer summer that year. Similar correlations with the spring SAM are also observed for the summer maximum and minimum SAT (Figure 1(b) and (c)), implying a shift of the entire probability distribution of NEC summer SAT towards a warm state after a positive spring SAM phase. In addition, as shown in Figure 1(d)–(g), NEC summer precipitation and relative humidity are negatively correlated with the spring SAM, whereas sunshine duration is positively linked. These correlations indicate that NEC usually experiences less precipitation and more sunshine in summers when the spring SAM is positive, which further confirms the robustness of the relationship between NEC summer SAT and the spring SAM.

In view of the linear trends in the SAMI (Fogt *et al.*, 2009) and NEC summer SAT, the correlation coefficients in Figure 1(a)–(g) between undetrended variables may be dominated by their trends. Therefore, we redo Figure 1(a)–(g) using detrended variables (not shown), and the detrended correlations are generally in agreement with that in Figure 1(a)–(g), which further verifies the connections between the spring SAM and NEC summer climate on interannual scale.

The area-averaged SAT over NEC (115–135°E, 40–50°N) from 38 weather stations is defined as the NEC temperature index (NECTI). Figure 1(h) shows the normalized time series of the summer NECTI and the spring SAMI. The temporal variations of these two indices are generally consistent with each other. The correlation between them is 0.44 (significant at the 99% confidence level). In addition, the detrended time series are also shown in Figure 1(h), and their out-of-phase relationship is still evident on interannual scale. The correlation between the detrended series is 0.34 (significant at the 95% confidence level), indicating that the positive correlation between the spring SAM and summer NECTI is not just a reflection of their linear trends. Figure 1(i) illustrates the leading correlation between the SAM and summer NECTI, and the most significant correlation exists when the SAM leads the summer NCETI by 1 to 3 months.

The NAM and ENSO are also important signals that may influence the NH regional climate. The correlation between the spring NAMI, spring Niño 3.4 index, and the summer NECTI are 0.17 and −0.30, respectively, which are weaker than that between the spring SAMI

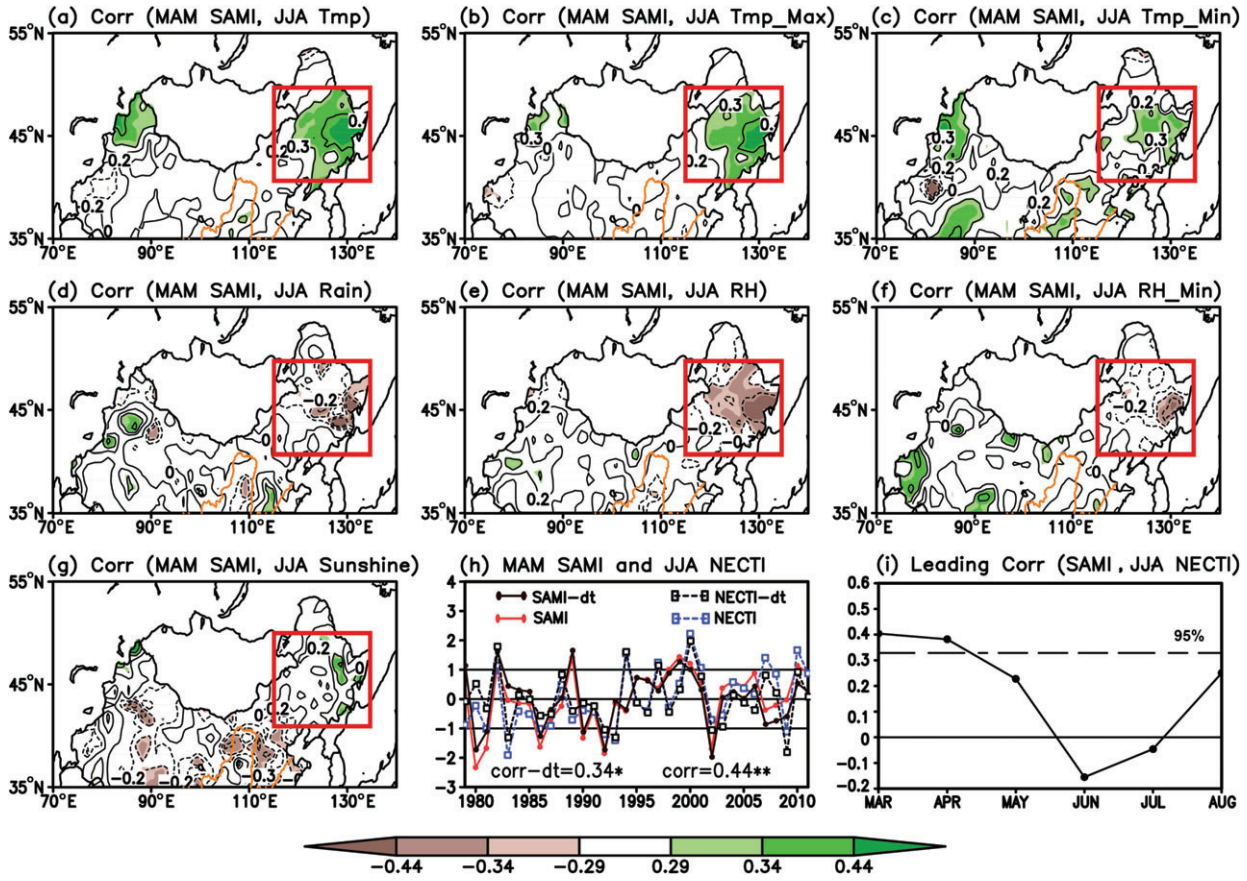

Figure 1. Maps of correlation between the boreal spring (MAM) SAMI and seasonal average summer (JJA) meteorological elements (a)–(g) over northern China for the period 1979–2011. (a) Daily mean surface air temperature (SAT); (b) daily maximum SAT; (c) daily minimum SAT; (d) precipitation; (e) daily mean relative humidity; (f) daily minimum relative humidity; and (g) sunshine duration. The contour interval is 0.1, and shadings from light to dark indicate the 90%, 95%, and 99% confidence levels. The domain of northeast China (NEC) is surrounded by the red solid lines. (h) Normalized time series of the spring SAMI (red solid line) and NEC summer temperature index (NECTI; blue dashed line). The black lines represent the detrended spring SAMI (solid) and summer NECTI (dashed). The symbols ** and * indicate significance at the 99% and 95% confidence levels, respectively. (i) Leading correlation coefficients between the SAMI from March to August, and the summer NECTI. The dashed line indicates the 95% confidence level.

and the summer NECTI (0.44), implying that the spring SAM plays an important role in modulating the summer SAT in NEC.

Furthermore, as ENSO and the SAM show some covariability (Zhou and Yu, 2004; Gong *et al.*, 2013), partial correlation was used to exclude the possible effects of ENSO. The partial correlation between the spring SAM and summer NECTI after removing the spring ENSO is 0.39 (significant at the 95% confidence level), supporting the robustness of the relationship between the spring SAM and NEC summer SAT.

4. Corresponding physical processes

4.1. The boreal spring SAM and NEC summer radiation and circulation

As SAT is directly associated with cloud and radiation processes near the surface, if we are to understand the linkage between the spring SAM and NEC summer SAT, it is helpful to investigate connections between the spring SAM and NEC summer cloud and radiation processes.

Firstly, relationships between radiation variables and NEC summer SAT will be explored quantitatively. Specifically, area-averaged summer TCDC, NSWRF, and NLWRF over NEC (115–135°E, 40–50°N) were calculated as indices, and the correlation matrix of these indices and the NECTI is shown in Table 1. The correlation between area-averaged TCDC and NSWRF, NSWRF and NLWRF, NLWRF and NECTI are −0.95, 0.98, and 0.54, respectively. These relationships can be interpreted according to the radiation processes; i.e. decreases in TCDC usually lead to increases in incoming NSWRF arriving at the land, which is expected to heat the ground and hence result in more outgoing NLWRF, and the enhanced NLWRF could further warm local SAT.

Secondly, relationships between the spring SAM and summer radiation variables are illustrated in Figure 2(a)–(c), which shows the composite differences in summer TCDC, NSWRF, and NLWRF between high and low spring SAMI years for the period 1948–2011. As shown in Figure 2(a), NEC summer TCDC is negatively linked to the spring SAM, implying

Table 1. Correlation matrix of the boreal summer NECTI, and the regional average TCDC, NSWRF, and NLWRF over 115–135°E, 40–55°N for the period 1979–2011.[a]

	NSWRF	NLWRF	NECTI
TCDC	-0.95^{**} (-0.92)	-0.92^{**} (-0.88^{**})	-0.67^{**} (-0.54^{**})
NSWRF		0.98^{**} (0.96^{**})	0.63^{**} (0.49^{**})
NLWRF			0.54^{**} (0.38^{*})

[a]The values in brackets are the correlation coefficients for the detrended time series.
The symbols ** and * indicate significance at the 99% and 95% confidence levels, respectively.

that when the spring SAM is in a positive phase, NEC summer cloudiness generally declines. According to the previous analysis, decreases in TCDC are associated with increased NSWRF and NLWRF over NEC. Therefore, the NSWRF and NLWRF are expected to be positively linked with the SAM. Figure 2(b) and (c) illustrates that a positive correlation between the spring SAM and summer NSWRF and NLWRF is evident over NEC. Figure 2(d) shows the normalized time series of the summer area-averaged TCDC, NSWRF, NLWRF, and the summer NECTI, and the correlation among the summer radiation variables and the summer NECTI is well defined.

Thirdly, circulation anomalies responsible for the linkage between the spring SAM and summer radiation variables were examined. Figure 3(a) illustrates the composite differences in the NH summer geopotential height between high and low spring SAMI years. The positive spring SAM is associated with high-pressure anomalies over East Asia. Besides, the composite analysis in Figure 3(a) was repeated after excluding the ENSO signal (not shown), and the summer high-pressure anomalies in East Asia are still evident. Furthermore, the composite difference in wind and vertical velocity at 850 hPa (Figure 3(b)) shows that when the spring SAM is in a positive phase, there is usually a stronger sinking motion over the East Asian middle latitudes in summer. This is likely to impede the formation of cloud, which will influence local radiation processes and lead to a warmer SAT.

4.2. The role of NIO SST

What is the physical process that connects the spring SAM to the East Asian summer circulation? As Nan *et al.* (2009) suggested, one underlying factor may involve the Indian Ocean SST acting as an oceanic bridge. Figure 4(a) shows the composite differences in summer SST between high and low spring SAM years. It can be seen that the boreal spring SAM is actually correlated with NIO summer SST, which is in agreement with that in the study by Nan *et al.* (2009). We further verify the role of NIO SST in regulating East Asian circulation.

Firstly, diagnostic analyses are employed to detect association between the summer NIO SST and East Asian circulation. An NIO SST index is defined as the regionally averaged SST over the key region (60–100°E, 5–15°N). Figure 4(b) and (c) shows the composite differences in geopotential height, horizontal wind, and vertical velocity between warm and cold NIO SST years. As shown in Figure 4(b), warmer NIO SST relates to higher pressure over East Asia, which is very similar to that in Figure 3(a), indicating strongly that the NIO SST is a key factor that links the spring SAM with summer air pressure anomalies over East Asia. Furthermore, Figure 4(c) shows that warmer NIO SST is also linked to an anomalous anticyclonic circulation and sinking motion, thus resulting in a decrease in cloudiness and warmer NEC summer SAT.

Secondly, a physical process is provided to understand the influence of summer NIO SST on East Asian circulation. Figure 4(d) illustrates the climatology of summer geopotential height at 850 hPa (contours). The Asian continent is covered by low pressure in summer, which is an action center of the atmosphere, and its generation is associated with the thermal contrast between the warmer-continent and cold-ocean. An Asian continent low pressure (AL) index is defined as regional averaged geopotential height at 850 hPa over the region (80–130°E, 40–60°N). The correlations between the AL index and SST are shown in Figure 4(d) (shadings). It is evident that the AL index is significantly related to the NIO SST. Warmer NIO SST corresponds to weaker air-sea thermal contrast in summer, and thus leading to a weaker AL and higher pressure anomalies over East Asia.

To further elaborate the covariablity between the NIO SST and East Asian circulation, the SVD analysis is applied to the geopotential height and SST over the domain (40–150°E, 0–70°N). The leading heterogeneous SVD modes are shown in Figure 4(e), which accounts for 52% (above the noise level) of the total squared covariance. The leading modes in Figure 4(e) imply that a warmer NIO SST is associated with higher geopotential heights over East Asia, which is in conformity with the conclusions from Figure 4(b)–(d) and confirms further the linkage between summer NIO SST and East Asian circulation.

Therefore, summer NIO SST may be regarded as an important bridge through which the spring SAM can regulate NEC summer SAT.

5. Discussion and conclusions

This paper has examined how the boreal spring SAM might influence NEC summer SAT. The positive spring SAM leads to an abnormal anticyclonic circulation and descending air over NEC through NIO SST. The sinking motion reduces local cloudiness, which is believed to alter levels of incoming solar radiation in such a way as to increase outgoing longwave radiation and so warm the SAT. This implies that the climatic impacts of the SAM can even extend to the NH middle latitudes.

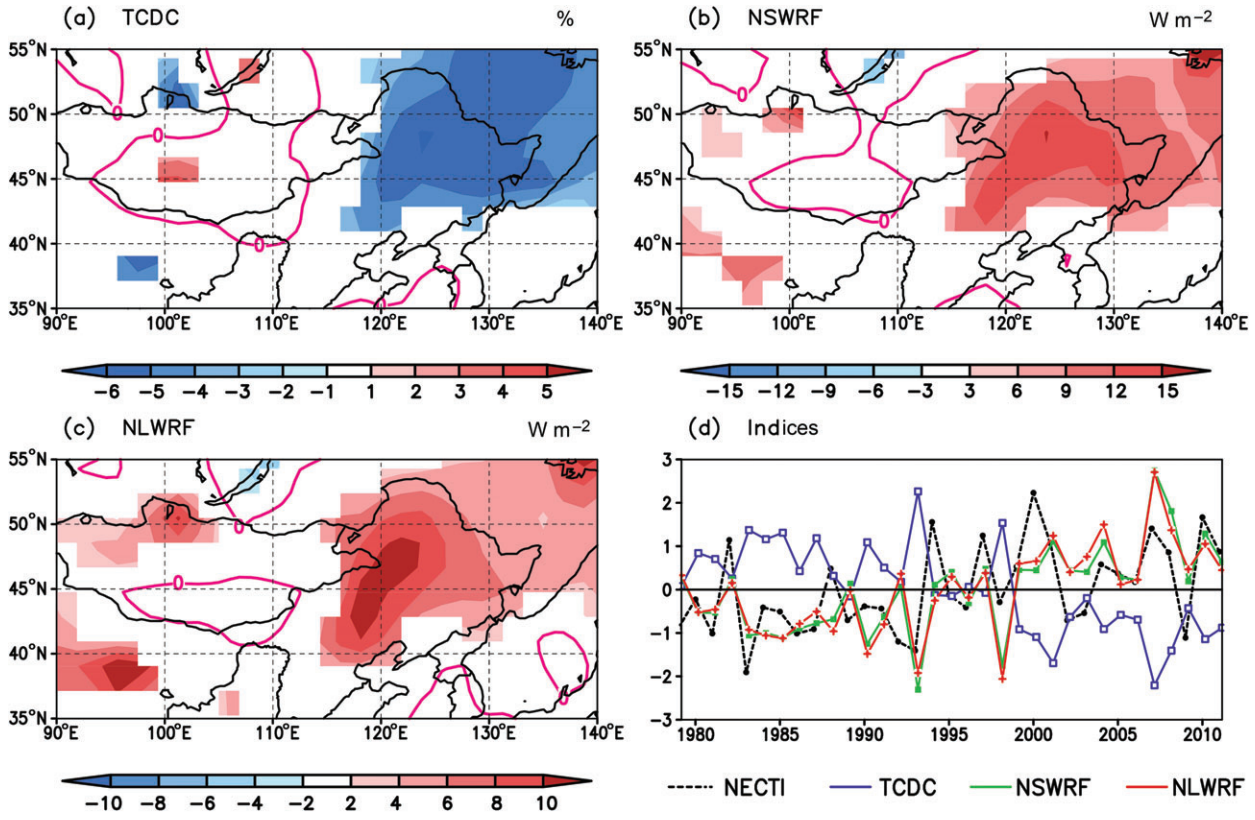

Figure 2. Composite differences in summer between high and low boreal spring SAMI years for the period 1948–2011 for (a) total cloud cover (TCDC, %), (b) net shortwave radiative flux (NSWRF, W m^{-2}), and (c) net longwave radiative flux (NLWRF, W m^{-2}). The high and low SAM years were selected based on the fluctuations of the SAMI beyond one standard deviation. Only values significant at the 90% confidence level are shown. (d) Normalized time series of NECTI, regional average TCDC, NSWRF, and NLWRF over 115–135°E, 40–55°N for the period 1979–2011 (The NECTI based on station observation data only covers the period 1979–2011).

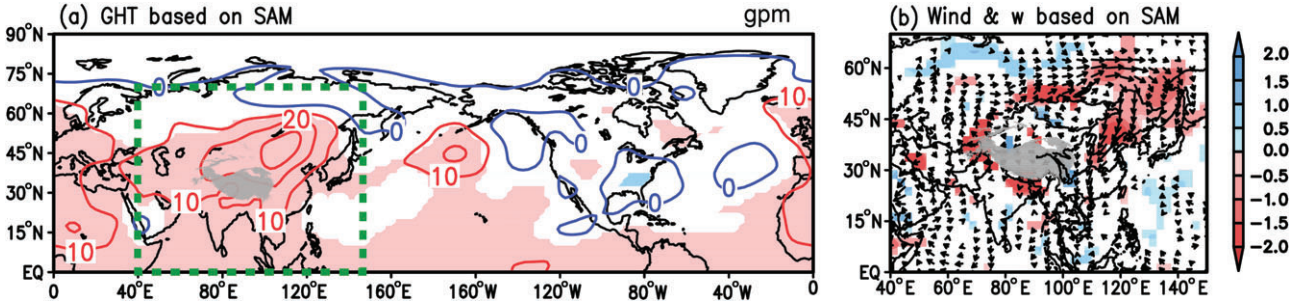

Figure 3. Composite differences in summer circulation between high and low spring SAM years for the period 1948–2011. (a) Geopotential height (contours, gpm) at 850 hPa. Color shading indicates significance at the 90% confidence level, and the region that we mainly focus is surrounded by the green dashed line (40–150°E, 0–70°N). (b) Wind (vectors, m s^{-1}) and vertical velocity (shaded, 6×10^{-3} Pa s^{-1}) at 850 hPa. Only values significant at the 90% confidence level are shown. The gray shading is the Tibetan Plateau.

This influence of the spring SAM on NEC summer SAT has implications for downscaled seasonal predictions. A simple seasonal prediction model for NEC summer SAT based on the spring SAMI was established (Figure S1). The concordance ratio of the signs between the observations and hindcast NECTI is up to 70% (Figure S1), providing direct evidence for that the spring SAM is a potential predictor for NEC summer SAT prediction.

Furthermore, we have explored the role of NIO SST as the pathway transmitting the influence of the spring SAM to NEC. We have found that the spring SAM is also significantly associated with summer SST over central tropical Pacific, and the SST anomaly pattern associated with the SAM shows the 'ENSO-like' characteristics (not shown). In view of the summer SST over this region linked to NEC summer SAT (not shown), the role of the tropical Pacific may also be crucial in linking the spring SAM on summer NEC SAT, and the NIO SST may be not the only way of transmitting the SAM signal to NEC. Considering the tropical Pacific SST, especially the ENSO, is important for regulating

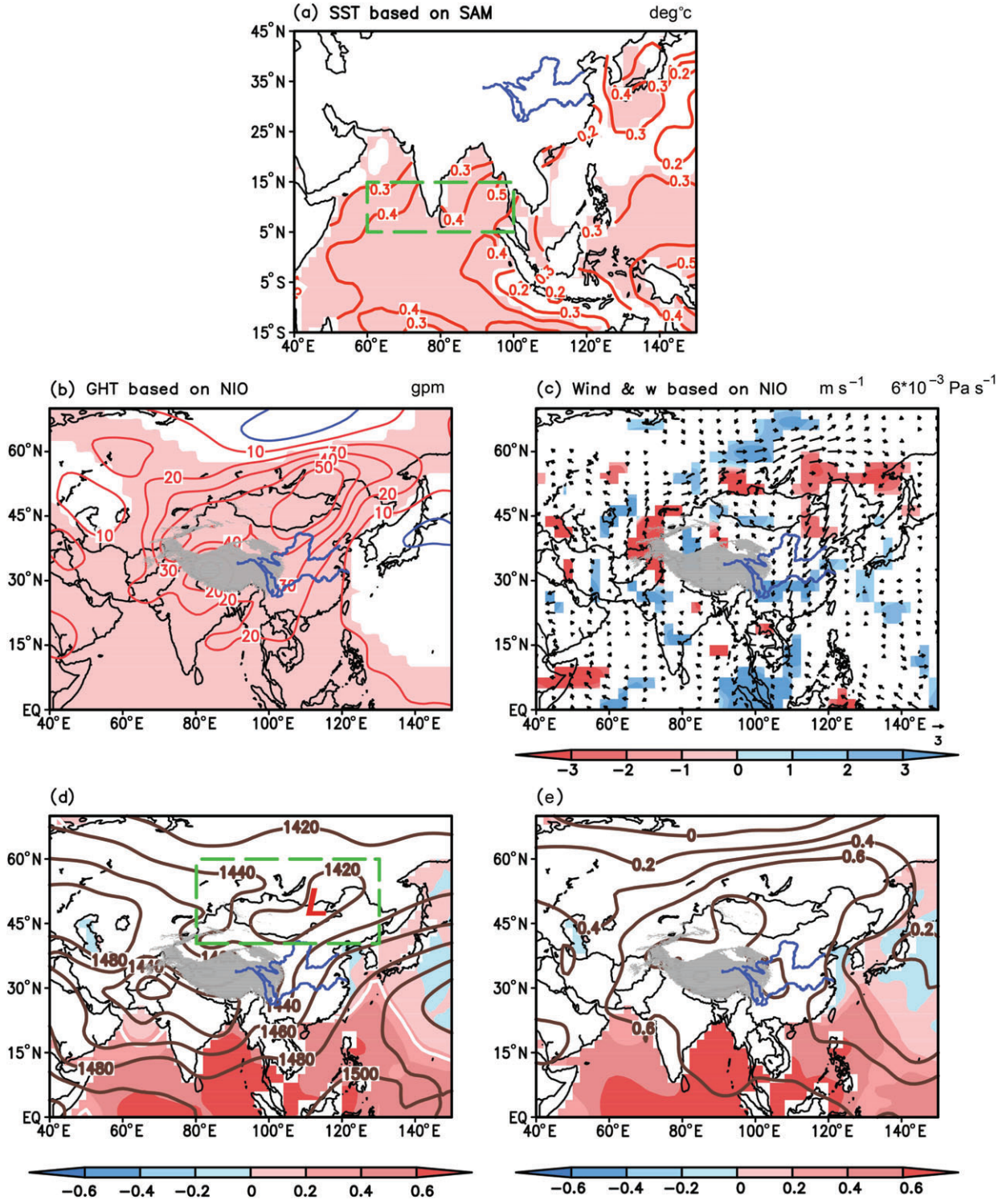

Figure 4. (a) Composite differences (°C) in summer sea surface temperature (SST) between high and low spring SAM years for the period 1948–2011. Color shading indicates significance at the 95% confidence level. The domain (60–100°E, 5–15°N) which is used to calculate the NIO SST index is surrounded by the green dashed line. The panels (b) and (c) are as in Figure 3(a) and (b), but based on the warm and cold Northern Indian Ocean (NIO) SST years. The warm and cold NIO SST years are selected based on the fluctuations of the summer NIO SST index beyond one standard deviation. (d) The brown contours denote climatology of summer geopotential height (gpm) at 850 hPa. The shadings represent correlation between the Asian continent low pressure (AL) index and sea surface temperature (SST), and the white contours denote the 95% confidence level. The domain (80–130°E, 40–60°N) which is used to calculate the AL index is surrounded by the green dashed line. (e) The leading heterogeneous singular value decomposition (SVD) modes for summer geopotential height (contours) and SST (shadings) over the region (40–150°E, 0–70°N). The gray shadings are the Tibetan Plateau.

East Asian circulation, we will investigate the role of tropical Pacific SST in the future.

As shown in Figure 3, patterns in high-pressure anomalies associated with the spring SAM are also evident over Northern North America, which locates between 45 and 60°N, i.e., almost the same as NEC. Correspondingly, a significantly positive correlation also exists between the spring SAM and summer air temperature over northern North America (Figure S2). This suggests that broader connections between the spring SAM and summer SAT in the NH may exist, and additional studies are needed to extend our understanding of these connections.

Acknowledgements

This work was jointly supported by the China Special Fund for Meteorological Research in the Public Interest (GYHY201306031), the 973 Program (2013CB430200), and the NSFC Key Project (41030961). Dr Robin Clark was supported by the Joint DECC/Defra Met Office Hadley Centre Climate Programme (GA01101). Thanks to the editor Dr Arthur J. Miller and the two anonymous reviewers for their comments and suggestions that helped us to improve the manuscript.

Supporting information

The following supporting information is available:

Figure S1. Observed and model estimated NECTI.

Figure S2. Relationship between the spring SAM and Northern North America summer circulation and air temperature.

References

Choi KS, Wang B, Kim DW. 2012. Changma onset definition in Korea using the available water resources index and its relation to the Antarctic oscillation. *Climate Dynamics* **38**: 547–562.

Ciasto LM, Thompson DWJ. 2008. Observations of largescale ocean–atmosphere interaction in the Southern Hemisphere. *Journal of Climate* **21**: 1244–1259.

Fogt RL, Perlwitz J, Monaghan AJ, Bromwich DH, Jones JM, Marshall GJ. 2009. Historical SAM variability. Part II: Twentieth-century variability and trends from reconstructions, observations, and the IPCC AR4 models. *Journal of Climate* **22**: 5346–5365.

Gong DY, Wang SW. 1999. Definition of Antarctic Oscillation index. *Geophysical Research Letters* **26**: 459–462.

Gong TT, Feldstein SB, Luo DH. 2013. A simple GCM study on the relationship between ENSO and the Southern Annular Mode. *Journal of the Atmospheric Sciences* **70**: 1821–1832.

He JH, Wu ZW, Jiang ZH, Miao CS, Han GR. 2007. Climate effect of the northeast cold vortex and its influences on Meiyu. *Chinese Science Bulletin* **52**: 671–679.

Ho CH, Kim JH, Kim HS, Sui CH, Gong DY. 2005. Possible influence of the Antarctic Oscillation on tropical cyclone activity in the western North Pacific. *Journal of Geophysical Research* **110**: D19104.

Li JP, Wang JXL. 2003. A modified zonal index and its physical sense. *Geophysical Research Letters* **30**: 1632, doi: 10.1029/2003GL017441.

Marshall GJ, Stott PA, Turner J, Connolley WM, King JC, Lachlan-Cope TA. 2004. Causes of exceptional atmospheric circulation changes in the Southern Hemisphere. *Geophysical Research Letters* **31**: L14205.

Nan SL, Li JP. 2003. The relationship between the summer precipitation in the Yangtze River valley and the boreal spring Southern Hemisphere annular mode. *Geophysical Research Letters* **30**: 2266, doi: 10.1029/2003GL018381.

Nan SL, Li JP, Yuan XJ, Zhao P. 2009. Boreal spring Southern Hemisphere Annular Mode, Indian Ocean sea surface temperature, and East Asian summer monsoon. *Journal of Geophysical Research* **114**: D02103.

Simpkins GR, Ciasto LM, Thompson DWJ, England MH. 2012. Seasonal relationships between large-scale climate variability and Antarctic sea ice concentration. *Journal of Climate* **25**: 5451–5469.

Sun JQ, Wang HJ, Yuan W. 2010. Linkage of the Boreal Spring Antarctic Oscillation to the West African Summer Monsoon. *Journal of the Meteorological Society of Japan* **88**: 15–28.

Thompson DWJ, Wallace JM. 2000. Annular modes in the extratropical circulation. Part I: Month-to-month variability. *Journal of Climate* **13**: 1000–1016.

Wu ZW, Li JP, Wang B, Liu XH. 2009. Can the Southern Hemisphere annular mode affect China winter monsoon? *Journal of Geophysical Research* **114**: D11107.

Wu RG, Yang S, Liu S, Sun L, Lian Y, Gao ZT. 2010. Changes in the relationship between Northeast China summer temperature and ENSO. *Journal of Geophysical Research* **115**: D21107.

Wu RG, Yang S, Liu S, Sun L, Lian Y, Gao ZT. 2011. Northeast China summer temperature and North Atlantic SST. *Journal of Geophysical Research* **116**: D16116.

Wu ZW, Jiang Z, Li JP, Zhong S, Wang L. 2012. Possible association of the western Tibetan Plateau snow cover with the decadal to interdecadal variations of Northern China heatwave frequency. *Climate Dynamics* **39**: 2393–2402.

Yuan XJ, Yonekura E. 2011. Decadal variability in the Southern Hemisphere. *Journal of Geophysical Research* **116**: D19115.

Zheng F, Li JP. 2012. Impact of preceding boreal winter southern hemisphere annular mode on spring precipitation over south China and related mechanism. *Chinese Journal of Geophysics* **55**: 3542–3557.

Zhou T, Yu RC. 2004. Sea-surface temperature induced variability of the Southern Annular Mode in an atmospheric general circulation model. *Geophysical Research Letters* **31**: L24206.

